STUDY OF CHANGES OF DISTANCE BETWEEN AXLES IN AUTOMOTIVE VEHICLES

OLIVEIRA, A.G, ademyr_go@eee.ufg.br
Universidade Federal de Goiás

Abstract. *This work will address the implications of structural changes of motor vehicles. Passenger vehicles are elongated transformed into cargo vehicles and limousines are stretched and a third axis is introduced. Whatever the change in the original distance between the front axle and rear axle, would necessarily involve changes in the vehicle's steering system to compensate for the differences in radii of curvature that appear when the vehicle executes a turn. As the steering system is standard maintained, the vehicles lost in driving change and may contribute to increased accident rates.*

Keywords: structural change vehicle; vehicular steering system.

1. INTRODUCTION

Structural modification of vehicles for changing the distance between the axles is relatively frequent in the following cases:

Case 1: Passenger vehicles are transformed into mini compact cars or large limousines, as shown in Fig. 1.

Figure 1: Limousine and mini car

Case 2: Specialty vehicles, as shown in Fig 1, are designed from parts of other vehicles, such as the buggy which are usually constructed from Volkswagen "fusca" or Volkswagen Brasilia.

Figure 2: Special Car, Buggy

Case 3: Cargo vehicles, as shown in Fig. 2, undergo lengthening the chassis to allow the installation of additional axes in order to accommodate wide loads or to give the vehicle greater load capacity.

Figure 3: Truck with 3 axles

Whatever the case, which is common in the interventions mentioned is that the original steering system of all vehicles are kept unchanged.

2. THE STEERING SYSTEM

The steering system is installed between the chassis and front suspension and is composed primarily of steering box, steering rods and joints. This system is responsible for the angle of the front wheels allowing the vehicle to follow a curved path, as shown in Fig. 4.

The front wheel has three angles: steering angle, the camber and caster (ROCKCRAWLER, 2010) as shown in Fig.5. These last two are introduced by the suspension and are directly related to the dynamic behavior of the vehicle and not the curvature of its trajectory.
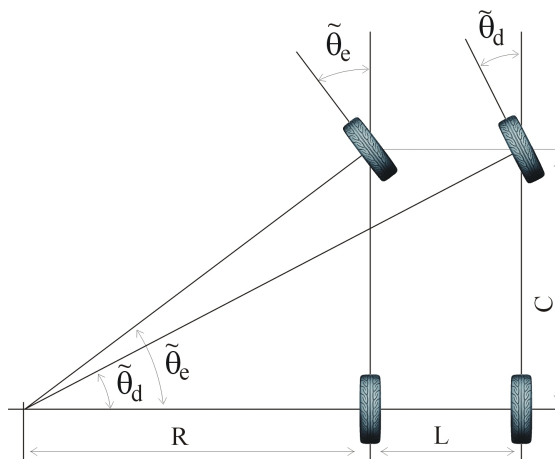

Figure 4: Angle of direction $\tilde{\theta}_e$ e $\tilde{\theta}_d$
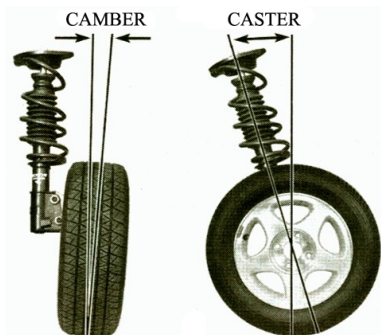

Figure 5: Angle camber e caster

In the geometric aspect, a vehicle that can describe a curved path requires that the front wheel left and right have different angles, respectively, and those that meet the following relationships:

$$\tilde{\theta}_e = \sin^{-1}(C/R) \tag{1}$$

and

$$\tilde{\theta}_d = \sin^{-1}(C/R+L) \tag{2}$$

where C is the wheelbase, R is the radius of the trajectory and L is the width of the vehicle.

The steering system can be modeled as symmetric two coupled four-bar mechanisms for the articulation of the steering box (HARTENBERGER, 1980) as shown in Fig. 6. In this case, for the vehicle in a straight trajectory, the pivot point is the midpoint of the width of the vehicle.
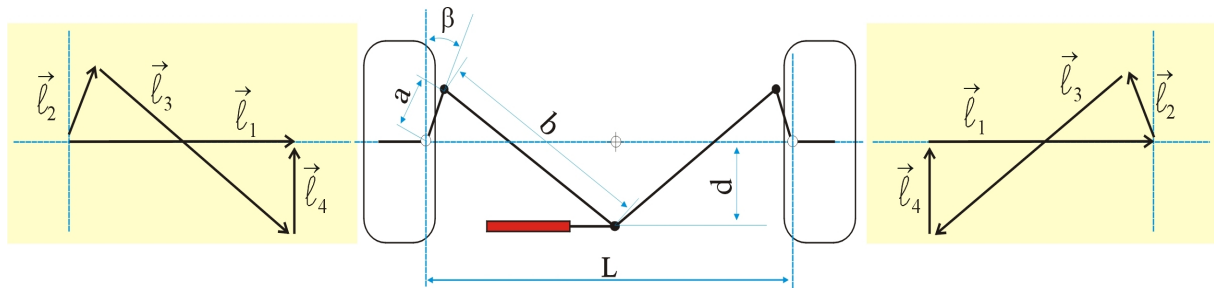

Figure 6: Model of steering system symmetrical: four-bar mechanism

The synthesis of algebraic four-bar mechanism (Norton, 2010) considers four vectors $\vec{l}_1$, $\vec{l}_2$, $\vec{l}_3$ e $\vec{l}_4$, with their respective angles θ_1, θ_2, θ_3 e θ_4. The angle β is design variable and adjusts the timing of compensation between the two four-bar mechanisms.

For a steering system equipped with steering box-type rack has the following configuration:

- $\vec{l}_1$ with module variable and $\theta_1 = 0$;
- $\vec{l}_2$ with module variable and θ_2 variable;
- $\vec{l}_3$ with constant modulus and θ_3 variable ;
- $\vec{l}_4$ with constant modulus and $\theta_4 = \pi/2$.

For the synthesis of algebraic mechanism should be reminded of the Euler vector notation which is given by

$$\vec{l} = l\cos(\alpha) + l\sin(\alpha) \tag{3}$$

and the following trigonometric relations:

$$\cos(\alpha) = \frac{1 - \tan^2(\alpha/2)}{1 + \tan^2(\alpha/2)} \tag{4}$$

and

$$\sin(\alpha) = \frac{2\tan^2(\alpha/2)}{1 + \tan^2(\alpha/2)} \tag{5}$$

2.1 – MECHANISM OF LEFT STEERING CAR

The four-bar mechanism on the left side of the steering system can be modeled as

$$\vec{l}_2 + \vec{l}_3 + \vec{l}_4 - \vec{l}_1 = 0 \tag{6}$$

Applying eq. (1) in eq. (6) and considering $\theta_4 = 90^o$ and $\theta_1 = 0^o$, obtains eq. (7). This equation gives the position of the middle joint of the steering system.

$$l_1 = l_2\cos(\theta_2) + \sqrt{l_2^2\cos^2(\theta_2) + l_3^2 - l_2^2 - l_4^2 - 2l_2l_4\sin(\theta_2)} \tag{7}$$

The width of l_3 is obtained for the initial conditions β , $l_1 = \dfrac{L}{2}$ e $\theta_2 = 0^o$ such that

$$l_3 = \sqrt{\left(\frac{L}{2} - l_2 \sin(\beta)\right)^2 + (-l_2 \cos(\beta) - l_4)^2} \tag{8}$$

2.1 – MECHANISM OF THE RIGHT SIDE OF STEERING SYSTEM

The four-bar mechanism on the right side of the steering system can be modeled as

$$\vec{l_1} + \vec{l_2} - \vec{l_3} - \vec{l_4} = 0 \tag{9}$$

Applying eq. (1), eq. (2) and eq. (3) in eq. (7) we obtain

$$\theta_2 = 2 \tan^{-1}(X) \tag{10}$$

where

$$X = \frac{-B \pm \sqrt{B^2 - 4AC}}{2A} \tag{11}$$

$$A = -l_1 - Q \tag{12}$$

$$Q = \frac{l2^2 - l_2^2 - l_1^2 - l_4^2}{-2 l_2} \tag{13}$$

$$B = 2 l_4 \tag{14}$$

$$C = l_1 - Q \tag{15}$$

The bars l_2 , l_3 e l_4 have equal lengths for the two mechanisms. If l_{1e} is the length of the bar l_1 of the left mechanism, then the bar l_1 of the right side of the mechanisms is such that

$$l_{1d} = L - l_{1e} \tag{16}$$

Observing Fig.4, the steering angle of the right front wheel is given by $\theta_d = \theta_2$, where θ_2 is given by eq. (8).

3. DESIGN VEHICLE STEERING MECHANISM

The development of a project steering mechanism of the following steps:

Step 1: given the values l_4 , L e C , established in the design of the vehicle;
Step 2: setting limits $\beta_{mínimo}$, $\beta_{máximo}$, $l_{2mínimo}$, $l_{2máximo}$ and the accepted tolerance. The value of l_3 is such that $l_3 = f(\beta, l_2)$.
Step 3: Assign a value of radius of curvature such that $R \geq R_{mínimo}$.
Step 4: Assign values to β e l_2 such that $\beta_{mínimo} \leq \beta \leq \beta_{máximo}$ and $l_{2mínimo} = l_2 \leq l_{2máximo}$.
Step 5: Calculate the values of θ_e by equations [1] and [9] . Calculate E_e , the magnitude of the error between the two values.
Step 6: Calculate θ_d by equations [2] and [11]. Calculate E_d ,, the modulus of the error between the two values.
Step 7: If the values of errors E_e and E_d is such that $E_d > tolerance$ ou $E_d > tolerance$, steps 4, 5, 6 and 7 should be repeated.
Step 8: If the valuers of the errors E_e and E_d is such that $E_e \leq tolerance$ e $E_d \leq tolerance$ then β and l_2 are values may be appropriate. Check all the values set in step 3.
The iterative process established in steps 4, 5, 6, 7 and 8 is very inefficient method of trial and error. In this case it is necessary to use an optimization algorithm (VANDERPLAST, 1999) as "the method of gradient descent".

In short, the gradient method is a descent optimization algorithm that uses first-order gradient of a function dependent variables to be optimized. This gradient allows to guide the growth of each design variable such that the function is taken to a maximum value or minimum.

4. RESULTS

Based on reverse engineering of the vehicle Volkswagen Brasilia obtained the following values: $L=1,55\,m$, $C=2,4\,m$, $l_4=0,15\,m$ e $\beta=5^0$.

A Fig. 7 shows is obtained with the aid of eq. (1) and eq (2). ($\tilde{\theta}_e=\sin^{-1}(C/R)$ e $\tilde{\theta}_d=\sin^{-1}(C/R+L)$) considering $L=1,55\,m$ e $C=2,4\,m$, for different values of curve radius, simulating a curve to the left, $R<0$, followed by curve toward the right side, $R>0$.
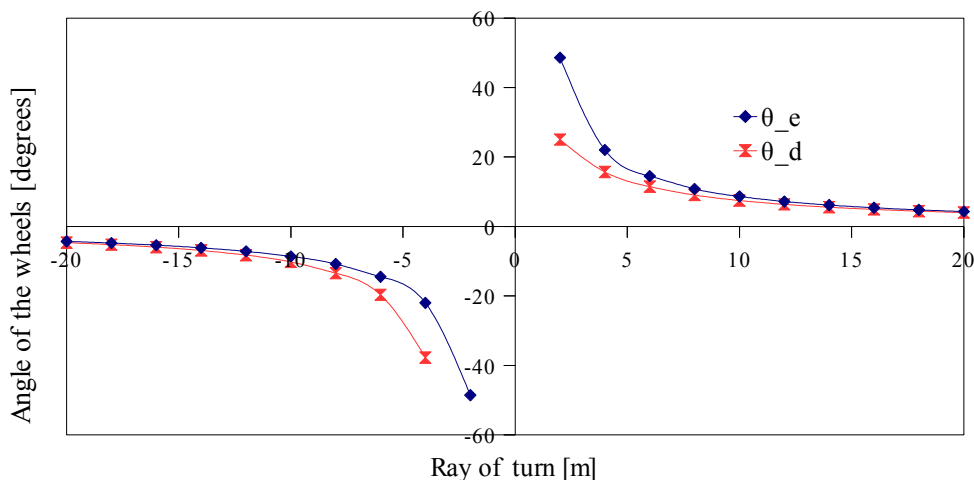

Figure 7: Angles $\tilde{\theta}_e$, $\tilde{\theta}_d$ as a function of R

The eq. (1) and eq. (2) can be combined such that

$$\tilde{\theta}_d=\sin^{-1}\left(\frac{C}{C/\sin(\tilde{\theta}_e)-L}\right) \tag{17}$$

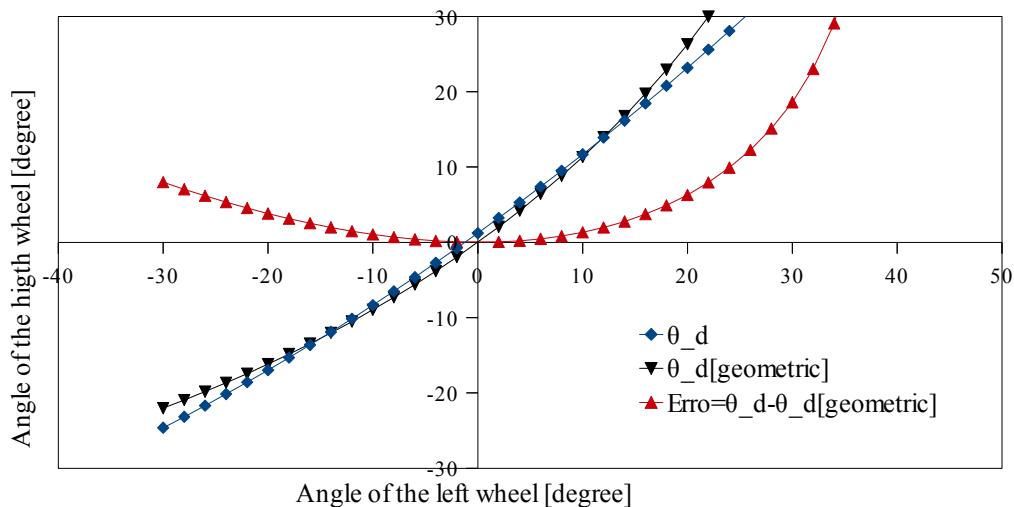Fig. 8 is obtained from eq. (17) for $L=1,55\,m$ e $C=2,4\,m$, for different values of R.

Figure 8:Angulo $\tilde{\theta}_e$ and $\tilde{\theta}_d$ as a function of the turning radius.

With the aid of eq. (5), eq. (8) and eq. (15) we obtain Fig. 9. This figure shows for $30^o < \tilde{\theta}_e < 30^o$, a comparison between $\tilde{\theta}_d$ and θ_d to $\tilde{\theta}_e = \theta_e$.
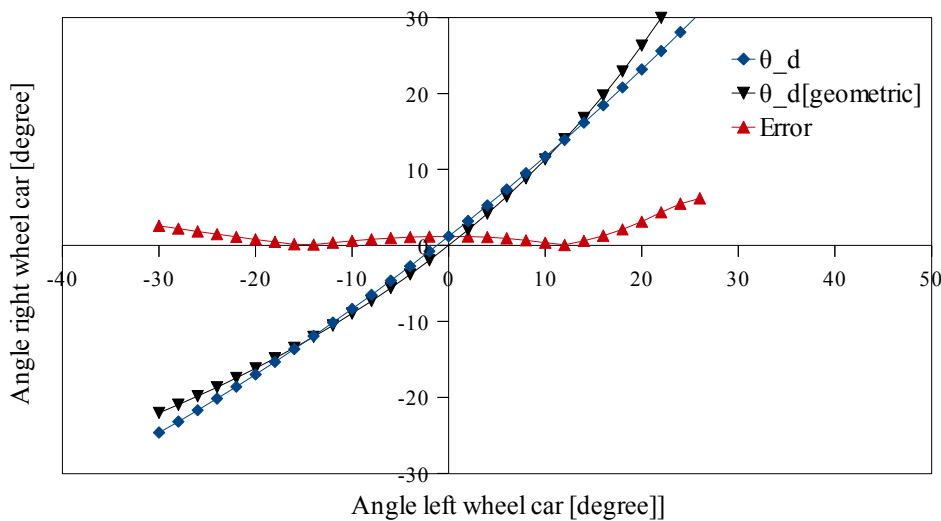

Figure 9: Comparison between $\tilde{\theta}_d$ and θ_d

Whereas the vehicle in question ($L = 1,55\,m$ e $C = 2,4\,m$) running a curve to the left such that $\theta_e = -14^0$, and the eq. (8) results $\theta_d = -12,02^0$. By varying the length of the distance between axles such that $1,5\,m \leq C \leq 4,5\,m$ and with the aid of eq. (8) gives the Fig.10.
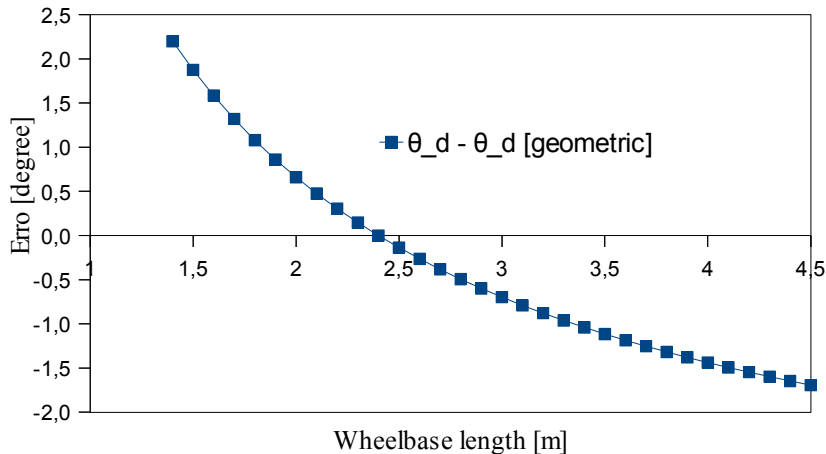

Figure 10:Convergence error.

4. CONCLUSIONS

Fig. 4 and Fig. 7 shows that for a vehicle run a curve, the front wheels left and right assume different angles. These angles are geometrically defined in terms of vehicle dimensions and the radius of the curve described by him.

The vehicular steering system consists of two four-bar mechanisms, adjusted for printing angle left wheel and right wheel, keeping necessary difference (as shown in Fig.8) for the vehicle to perform curvilinear trajectory. The design of a steering system is peculiar to the dimensions of the vehicle.

Fig. 9 shows that there is error values of geometric angles of the wheel and angle values imposed by the steering system.

Fig. 9 also shows that these errors are larger for larger values of angles, so for smaller radius curves.

This explains the characteristic noise of friction between the tread and the tire when the vehicle performs maneuvers in tight parking.

Fig. 9 also shows that for angles between $\pm 20^0$ matching range of major operation, this error is reduced to values close to $\pm 1^0$.

Fig. 10 shows that kept the original design of the steering system, changes in the wheelbase significantly affects the convergence error. Reducing the extent wheelbase introduces serious errors when compared with the increase of it. This explains how unstable is the direction of most buggies when they are traveling on asphalt floor. When one travels on the track buggy off-road, this effect is not observable since the sand or dirt floors absorb the errors of convergence.

5. BIBLIOGRAPHY

HARTENBERG, R. S. ; DENAVIT, J., *Kinematic Synthesis of Linkages*, McGraw-Hill, New York, 1980.
NORTON, R. L. Cinemática e dinâmica dos mecanismos. ed. Bookman. 2010. 800 p. ISBN: 9788563308191.

ROCKCRAWLER: TECH REPORTS and Reviews. Available at <http://www.rockcrawler.com/ techreports/ index.asp>. Accessed at 15 dez. 2010.

SHIGLEY, J.E.; MISCHKE, C.R.; BUDYNAS, R.G. Projeto de engenharia mecânica. 7.ed. Porto Alegre: Bookman, c2005. 960 p., il. ISBN 978-85-363-0562.

VANDERPLAATS, G.N. Numerical optimization techniques for engineering design. 3. ed. Colorado Springs, CO: Vanderplaats Research and Development, 1999. 441 p. ISBN 0-944956-00-9.